The Plant Cell, Vol. 11, 2013–2030, October 1999, www.plantcell.org © 1999 American Society of Plant Physiologists

Magnaporthe grisea Pth11p Is a Novel Plasma Membrane Protein That Mediates Appressorium Differentiation in Response to Inductive Substrate Cues

Todd M. DeZwaan, Anne M. Carroll, Barbara Valent, and James A. Sweigard[1]

Dupont Agricultural Enterprise, E.I. du Pont de Nemours and Company, Inc., P.O. Box 80402, Wilmington, DE 19880-0402

Mutagenesis of *Magnaporthe grisea* strain 4091-5-8 led to the identification of *PTH11*, a pathogenicity gene predicted to encode a novel transmembrane protein. We localized a Pth11–green fluorescent protein fusion to the cell membrane and vacuoles. *pth11* mutants of strain 4091-5-8 are nonpathogenic due to a defect in appressorium differentiation. This defect is reminiscent of wild-type strains on poorly inductive surfaces; conidia germinate and undergo early differentiation events, but appressorium maturation is impaired. Functional appressoria are formed by *pth11* mutants at 10 to 15% of wild-type frequencies, suggesting that the protein encoded by *PTH11* (Pth11p) is not required for appressorium morphogenesis but is involved in host surface recognition. We assayed Pth11p function in multiple *M. grisea* strains. These experiments indicated that Pth11p can activate appressorium differentiation in response to inductive surface cues and repress differentiation on poorly inductive surfaces and that multiple signaling pathways mediate differentiation. *PTH11* genes from diverged *M. grisea* strains complemented the 4091-5-8 *pth11* mutant, indicating functional conservation. Exogenous activation of cellular signaling suppressed *pth11* defects. These findings suggest that Pth11p functions at the cell cortex as an upstream effector of appressorium differentiation in response to surface cues.

INTRODUCTION

Fungal pathogens of plants undergo infection-specific differentiation in response to distinct host physical and chemical cues (Kolattukudy et al., 1995). For example, the bean rust *Uromyces appendiculatus* forms an infection structure upon encountering ridges that are the height of stomatal guard cells (Hoch et al., 1987), whereas the avocado pathogen *Colletotrichum gloeosporioides* specifically forms an infection structure in the presence of waxes from avocado but not other plants (Podila et al., 1993). The filamentous ascomycete *Magnaporthe grisea* is the blast pathogen of many grass species, including rice. *M. grisea* provides an excellent system for studying pathogen differentiation in response to host cues because it is amenable to molecular and classical genetics, and the cytology of the host–parasite interaction is known in great detail (reviewed in Howard, 1994; Talbot, 1995).

Infection by *M. grisea* begins when a conidium lands on the host plant and forms a germ tube that quickly differentiates into an infection structure, or appressorium. Appressorium differentiation occurs in two phases. First, the germ tube apex hooks and swells, and apical vesicles polarize toward the substratum. These events appear to represent a "recognition phase" in which the fitness of the substrate is monitored before the commitment to appressorium morphogenesis (Bourett and Howard, 1990). During the second phase, continued swelling of the germ tube apex yields a symmetrical appressorium, a septum forms between the appressorium and the remainder of the germling, and appressorial melanization occurs (Bourett and Howard, 1990). Once mature, the appressorium generates enormous hydrostatic pressure that mediates direct penetration of a narrow penetration peg through the host cuticle and epidermal layer (Howard et al., 1991). Intracellular hyphae then ramify throughout the host tissue and form conidiophores that erupt through to the host surface and release conidia into the environment (Howard, 1994).

A hard contact surface is essential for appressorium formation in *M. grisea* (Xiao et al., 1994), but differentiation is contingent on substrate hydrophobicity and the solute composition of the surrounding microenvironment. *M. grisea* forms appressoria efficiently on hydrophobic surfaces or in the presence of soluble host cutin monomers, but on hydrophilic, chemically inert surfaces, germlings fail to proceed beyond the early recognition phase of appressorium differentiation (Lee and Dean, 1994; Gilbert et al., 1996). Either hydrophobicity or cutin monomers alone are sufficient to induce appressorium differentiation, suggesting that simultaneous

[1] To whom correspondence should be addressed. E-mail jim.sweigard@usa.dupont.com; fax 302-695-4509.

processing of these inductive cues is coordinated to mediate differentiation (Choi and Dean, 1997).

Mutations in the Gα subunit homolog encoded by the *MAGB* gene prevent appressorium development beyond the recognition phase of differentiation (Liu and Dean, 1997). Thus, substrate sensing in *M. grisea* appears to be mediated by heterotrimeric G protein–coupled receptors that detect surface cues and transduce this information to one or more downstream signaling pathways. The Gα subunit protein encoded by the *MAGB* gene (MagBp) may activate cAMP-mediated signaling because exogenous cAMP suppresses the appressorium defect of *magB* mutants (Liu and Dean, 1997). Exogenous cAMP also supports appressorium differentiation in the absence of inductive cues, and *mac1* adenylate cyclase mutants have a defect in appressorium differentiation similar to that of *magB* mutants (Choi and Dean, 1997; Adachi and Hamer, 1998). However, *magB* mutants fail to differentiate on hydrophobic surfaces but continue to respond to soluble cutin monomers (Liu and Dean, 1997), whereas *mac1* mutants fail to differentiate in response to either inductive cue (Choi and Dean, 1997). Thus, parallel pathways of sensory input appear to converge at or before the *MAC1*-encoded adenylate cyclase protein (Mac1p) (Choi and Dean, 1997); however, little is known regarding the upstream effectors of these pathways.

The *M. grisea* fungal hydrophobin encoded by *MPG1* has been shown to play an upstream role in activating appressorium differentiation (Talbot et al., 1996). However, hydrophobins are secreted proteins that spontaneously aggregate at the cell periphery to form a hydrophobic surface layer (reviewed in Kershaw and Talbot, 1998), so Mpg1p is unlikely to interact directly with signaling components in the *M. grisea* cytoplasm. Mpg1p may mediate attachment of germlings to hydrophobic surfaces in a way that acts as a conformational cue for appressorium differentiation (Beckerman and Ebbole, 1996; Kershaw and Talbot, 1998).

Here, we describe *PTH11*, a pathogenicity gene encoding a novel transmembrane protein that is an upstream effector of appressorium differentiation. A Pth11–green fluorescent protein (GFP) fusion localizes to the cell membrane, and *pth11* mutants fail to progress beyond the recognition phase of appressorium differentiation, resulting in a loss of pathogenicity. Exogenous cAMP and diacylglycerol suppress defects associated with *pth11* mutants. cAMP restores both appressorium formation and pathogenicity, whereas diacylglycerol only restores appressorium formation. These findings suggest that the protein encoded by *PTH11* (Pth11p) plays an upstream role in activating appressorium signaling, possibly by acting as a receptor for inductive substrate cues. Analysis of *pth11* mutants of five distinct strains of *M. grisea* provided further evidence of an upstream signaling role for Pth11p. Furthermore, this analysis revealed that Pth11p could both activate differentiation in response to inductive surface cues and repress differentiation on poorly inductive surfaces. These results also suggested that the relative contribution of multiple signaling pathways to appressorium differentiation varies considerably among closely related strains of *M. grisea*.

RESULTS

Isolation of *M. grisea* Pathogenicity Mutants

We previously described a transformation-based insertional mutagenesis screen to isolate *M. grisea pth* mutants with altered pathogenicity (Sweigard et al., 1998). We performed this screen with the weeping lovegrass and barley pathogen 4091-5-8. Insertion mutants of 4091-5-8 were generated by restriction enzyme–mediated integration (REMI) of a linearized plasmid (pCB1004) carrying the hygromycin phosphotransferase gene (*HPH*) that confers hygromycin resistance (Carroll et al., 1994). Preliminary screening of 5538 transformants revealed 18 *HPH*-tagged *pth* mutants. We subsequently examined these mutants for the ability to cause disease on barley plants in a standard infection assay and found reproducible phenotypes ranging from no detectable symptoms to near wild-type levels of disease. Two *pth* mutants that formed rare disease lesions carried independent mutations in the same gene, which we designated *PTH11*. We refer to these mutants as K261 and K364 because both are products of a KpnI REMI transformation. When we crossed strains K261 and K364 to a wild-type strain of the opposite mating type (4136-4-3), the pathogenicity defect cosegregated as a single gene with the *HPH* marker used for insertional mutagenesis (Sweigard et al., 1998). This indicated that the pathogenicity defect of these strains was due to insertion of the *HPH* marker exclusively at the *PTH11* locus.

The pathogenicity defect of *pth11* mutants is shown in Figure 1. Standard infection assays were performed with strains 4091-5-8 (Figure 1A), K261 (Figure 1B), and K364 (data not shown). We assessed the pathogenicity of each strain according to the leaf lesion–type scale of Valent et al. (1991). When seedlings of the susceptible barley cultivar Bonanza were inoculated with the wild-type strain 4091-5-8, the plants became severely diseased. Large, spreading type 4 and type 5 lesions comprised the main body of the infected tissue, whereas smaller type 2 and type 3 lesions occurred at the periphery of the infection site (Figure 1A). In contrast to 4091-5-8, inoculation of barley seedlings with the *pth11* mutants K261 and K364 rarely resulted in the formation of disease lesions, and the seedlings continued to thrive as well as mock-inoculated plants (Figure 1B and data not shown). Occasionally, lesions formed on seedlings infected with *pth11* mutants that were comparable in size and appearance with the type 2 lesions found at the periphery of wild-type infection sites (Figure 1B). One explanation for these rare lesions is that the *pth11* mutant phenotype is unstable and bypass suppressor mutations occur at a high frequency. This has been observed previously in studies with

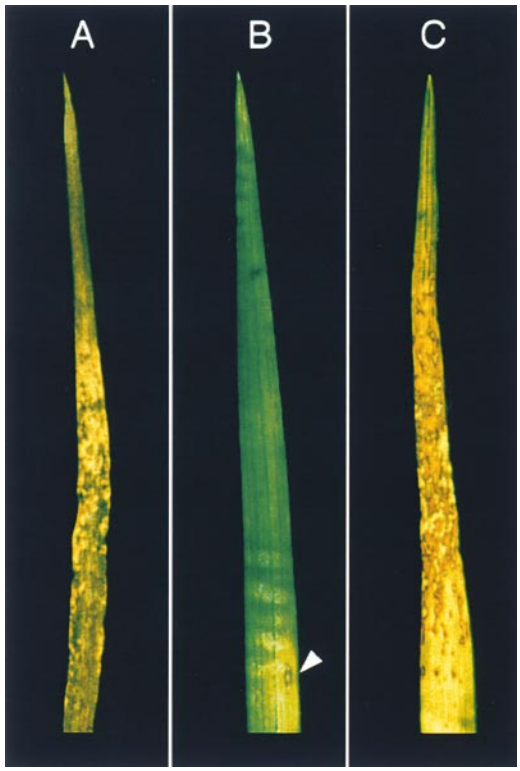

Figure 1. Barley Infection Assays.

Barley plants (cv Bonanza) were spray inoculated with conidial suspensions, and representative leaves were collected 5 days after inoculation and photographed. The arrowhead in **(B)** indicates a rare type 2 lesion that formed on plants inoculated with K261. Results identical to those shown in **(B)** and **(C)** were observed when plants were inoculated with the *pth11* mutant K364 and K364 transformed with pCB1272, respectively.

(A) Plants spray inoculated with wild-type strain 4091-5-8.

(B) Plants spray inoculated with *pth11* mutant strain K261.

(C) Plants spray inoculated with K261 transformed with the complementing *PTH11* plasmid pCB1272 (strain CP4154).

the *MAC1* adenylate cyclase gene of *M. grisea*. Under routine propagation, nonpathogenic *mac1* mutants acquired suppressor mutations that partially restored pathogenicity at a high frequency (Adachi and Hamer, 1998). To test for the presence of *pth11* suppressor mutations, we transferred conidia from rare disease lesions formed by strain K261 to oatmeal agar plates and allowed them to propagate into a conidial lawn. When we used these conidia to infect barley, we found that the *pth11* pathogenicity defect was retained, indicating that the rare lesions formed by *pth11* mutants were not due to suppressor mutations (data not shown).

We quantified the reduced virulence of *pth11* mutants by counting lesions produced on fully emerged cotyledons (see Methods). One hundred percent of the cotyledons inoculated with wild-type conidia were diseased, whereas only 20 to 30% of those inoculated with the *pth11* mutants showed any sign of disease. The mean lesion number per diseased cotyledon was 46.6 $\pm$ 22.8 lesions (n = 24 diseased cotyledons) for the wild-type strain 4091-5-8, 1.5 $\pm$ 0.8 lesions (n = 6 diseased cotyledons) for the *pth11* mutant strain K261, and 1.4 $\pm$ 0.8 lesions (n = 7 diseased cotyledons) for the *pth11* mutant strain K364. Thus, the mutants formed $\sim$25% of the wild-type number of diseased cotyledons and $\sim$3% of the wild-type number of lesions per diseased cotyledon. This translates to a level of virulence in *pth11* mutants that is $<$1% of the wild type (25% $\times$ 3% = 0.75%).

Characterization of Two Independent *pth11* REMI Mutations

Our strategy to characterize the REMI mutations in strains K261 and K364 was as follows. First, we recovered genomic DNA flanking the REMI site using the "plasmid rescue" method described by Sweigard et al. (1998). Next, we used this flanking DNA to probe a λ phage library constructed from wild-type 4091-5-8 genomic DNA. Genomic plasmids were then excised from hybridizing phage clones and transformed into K261 and K364 to test their ability to complement the pathogenicity defect of these strains. Subclones of complementing genomic plasmids were constructed to further elucidate the complementing activity. Finally, a subclone that complemented both K261 and K364 (pCB1303) and cDNA from the corresponding coding region was sequenced to identify the *PTH11* gene (Figures 2A and 2B). The rescued plasmids, complementing genomic clones, and genomic subclones are detailed in Figure 2A.

To identify the mutation in K261, we rescued plasmid pCB1621 from BglII-digested K261 genomic DNA. Because the REMI mutagenesis plasmid pCB1004 did not contain a BglII site, pCB1621 carried both 5′ and 3′ genomic regions flanking the REMI site. We used this flanking DNA to probe the 4091-5-8 genomic λ library and identified a complementing clone with a 13-kb insert (pCB1220). The complementing activity was then subcloned as a 4.7-kb HindIII fragment (pCB1278) (Figure 2A).

When we probed DNA gel blots with a genomic DNA fragment that included the 4.7-kb K261 complementing region, the probe hybridized to 4091-5-8 genomic DNA but failed to hybridize with K261 genomic DNA (Figure 3, lanes 1 and 2). This indicated that *PTH11* and the surrounding genomic region were deleted in strain K261. To define the boundaries of the deletion, we identified additional 4091-5-8 genomic clones using a *PTH11* cDNA probe (described below) and compared the sequences flanking the *PTH11* open reading frame (ORF) in these genomic clones with the insertion-flanking sequences in pCB1621. The sequence from the genomic clone pCB1399 showed identity to the insertion-flanking sequence at a point that was 4 kb upstream from the *PTH11* start site. This sequence also revealed a divergently

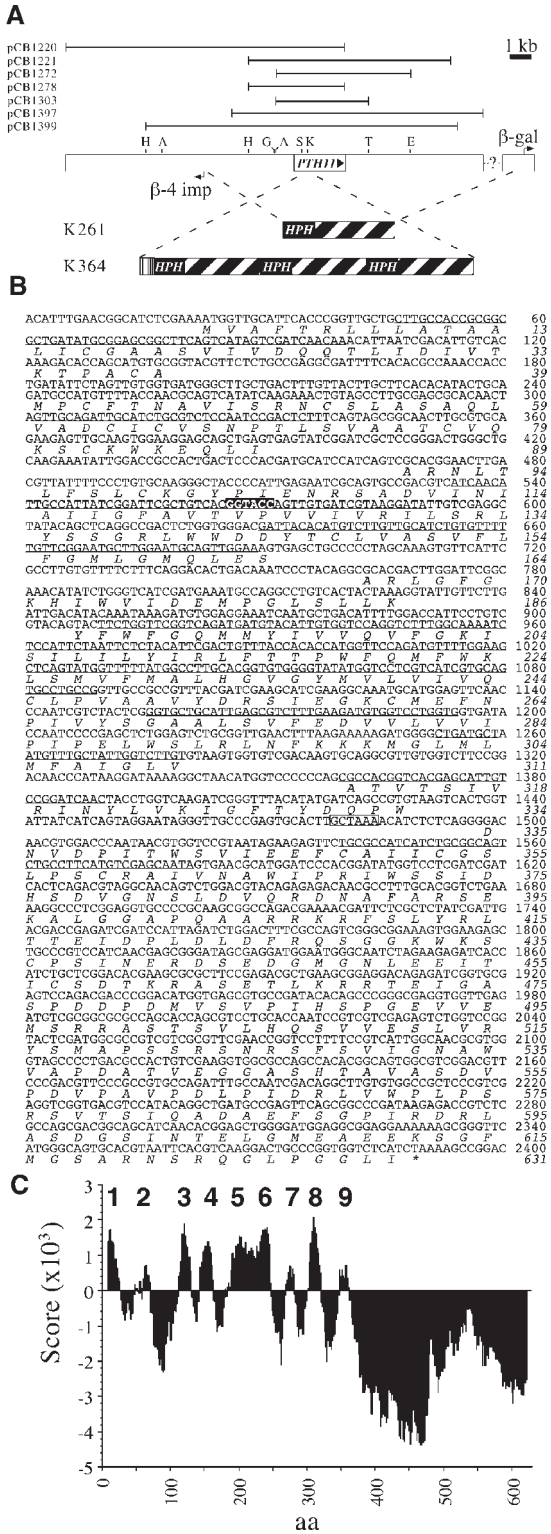

Figure 2. The *PTH11* Locus and Predicted Protein Structure.

(A) Summary of REMI events in *M. grisea* K261 and K364 and the transcribed ORF with homology to the β-4 subunit of importin from *Schizosaccharomyces pombe* that initiated 4.2 kb upstream from *PTH11* (Figure 2A). We were unable to define the 3′ deletion border of the K261 mutation, but the probe that failed to hybridize with K261 genomic DNA (Figure 3, lane 2) carried 4 kb of the *PTH11* downstream region. Sequence analysis of the 3′ insertion-flanking region in pCB1621 revealed the 5′ end of a β-galactosidase homolog (Figure 2A). Thus, the deletion in strain K261 extended at least 4 kb downstream from *PTH11* and included much of the region between *PTH11* and the β-galactosidase gene.

To identify the mutation in K364, we rescued the plasmid pCB1622 from K364 genomic DNA after digestion with BglII and BamHI. BamHI digested the REMI plasmid pCB1004 once, whereas BglII did not cut pCB1004. Thus, pCB1622 only carried the genomic region flanking one side of the insertion site. We used this insertion-flanking DNA to probe the 4091-5-8 genomic λ library and identified a complementing clone with a 9-kb insert (pCB1221). The K364 complementing activity was then subcloned as a 6.5-kb ApaI-

genomic clones described in this study. The *PTH11* ORF and surrounding genomic region are shown. The dashed lines indicate the insertion sites of the REMI plasmid pCB1004 in K261 and K364. The black and white hatching adjacent to the *HPH* gene represents pBC SK+ DNA that comprises the remainder of the REMI plasmid. The gray stippling at the 5′ end of the K364 insert represents ~0.7-kb of *M. grisea* mitochondrial DNA that was incorporated during REMI. The REMI event in K364 is shown with three tandem plasmid inserts, as described in the text. The 3′ HindIII site is not shown for pCB1278 because it originated from the pCB1220 polylinker. Restriction enzyme sites are abbreviated as follows: A, ApaI; E, EcoRI; G, BglII; H, HindIII; K, KpnI; S, SpeI; T, SstI. β-4 imp, β-4 subunit of importin; β-gal, β-galactosidase.

(B) Sequence and predicted translation of *PTH11. PTH11* genomic DNA sequence is shown. The highlighted region indicates the KpnI site at which the K364 REMI event occurred. The predicted protein translation is in italics below the DNA sequence. Gaps in the translation are introns. The boxed region in intron 6 indicates the unusual RCTRAA lariat site. Nucleotides that are predicted to encode membrane-inserted amino acids according to the TMpred program (Hofmann and Stoffel, 1993) are underlined. Although the second ATG at amino acid position 40 could feasibly serve as the start site, the region surrounding the start site shown fits the best consensus for *M. grisea* nuclear genes. In particular, the C residue at the −3 position of the second ATG was never observed in 29 genes, but the A at the −3 position of the first ATG was observed in 23 of the 29 genes.

(C) Prediction of Pth11p transmembrane regions. Hydropathy analysis was performed with the TMpred program (Hofmann and Stoffel, 1993; available at http://www.ch.embnet.org/software/TMPRED_form.html). Hydrophobic amino acids (aa) have scores greater than zero, whereas hydrophilic amino acids have scores less than zero. Nine predicted transmembrane regions are indicated.

EcoRI fragment (pCB1272) (Figure 2A). pCB1272 also complemented the pathogenicity defect of strain K261 (Figure 1C).

When we probed K364 genomic DNA gel blots with a fragment carrying *PTH11* and the surrounding region, the probe hybridized with two bands. One of these bands was also present in the wild type, whereas the other was shifted to a higher molecular weight than the corresponding wild-type band (Figure 3, lanes 1 and 3). This suggested that the mutation in K364 was due to an insertion in *PTH11* and not a gene deletion, as occurred in strain K261. We also performed DNA gel blot hybridization analysis with K364 genomic DNA digested with BglII and BamHI, using pCB1004 as a probe (Figure 3, lane 4). The hybridization analysis yielded two hybridizing bands; the 4.8-kb band was the same length as pCB1004. Thus, this band was composed only of plasmid DNA, whereas the 6.8-kb band was composed of plasmid and genomic DNA. This indicated that multiple copies of pCB1004 were tandemly incorporated at the *PTH11* locus in strain K364 during REMI. The intensity of the 4.8-kb plasmid DNA band appeared to be twofold greater than the band composed of plasmid and genomic DNA, suggesting that at least three copies of pCB1004 were incorporated (Figures 2A and 3, lane 4).

In addition to multiple copies of pCB1004, sequence analysis of the insertion-flanking region in pCB1622 revealed that 711 bp of mitochondrial DNA was incorporated into the genome of strain K364 during REMI (Figure 2A). We concluded that this DNA was mitochondrial on the basis of the following observations. First, the sequence encoded 159 amino acids that were 86% identical to a region of *Podospora anserina* cytochrome oxidase, a protein that is typically encoded by the mitochondrial genome. Second, in this sequence, the codon UGA encoded the amino acid tryptophan, as is common in mitochondrial genomes; UGA is a termination codon in nuclear-encoded genes. Finally, the introduction of mitochondrial DNA during nuclear integration events has been observed previously in ascomycetes (Scheistel et al., 1993). Alignment of the region adjacent to the mitochondrial DNA with the *PTH11* ORF (described below) revealed that insertion occurred at a unique KpnI site in *PTH11*, which is consistent with the use of KpnI for REMI during construction of strain K364 (Figures 2A and 2B).

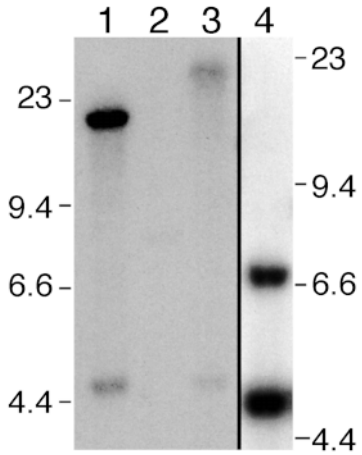

Figure 3. Wild-Type and *pth11* Mutant Genomic DNA Gel Blots.

Genomic DNA from the wild-type strain 4091-5-8 (lane 1) and the *pth11* mutants K261 (lane 2) and K364 (lanes 3 and 4) was digested with either ApaI (lanes 1 to 3) or BglII and BamHI (lane 4). The DNAs were then separated on agarose gels, and DNA gel blot transfers were performed according to Sambrook et al. (1989). Lanes 1 to 3 were probed with a 10.6-kb genomic fragment carrying *PTH11* that was generated by NotI-SfiI (polylinker sites) digestion of pCB1397. Lane 4 was probed with the REMI plasmid pCB1004. Numbers at left (lanes 1 to 3) and right (lane 4) indicate the position of λ HindIII DNA size standards in kilobases.

Identification of the *PTH11* Gene

We determined that mutation of the *PTH11* gene was responsible for the pathogenicity defect of both K261 and K364 as follows. First, the K261 and K364 complementing clones pCB1278 and pCB1272, respectively, carried the same gene. When we probed a cDNA library constructed from *M. grisea* 6043 (Sweigard et al., 1998) with the pCB1278 4.7-kb genomic DNA fragment, we identified three cDNA clones (pCB1312, pCB1313, and pCB1314); when we probed with the pCB1272 6.5-kb fragment, we identified one cDNA clone (pCB1315). Sequence analysis revealed that all four cDNAs were derived from *PTH11* (data not shown). Second, a 4.3-kb ApaI-SstI subclone (pCB1303) of pCB1272 complemented the pathogenicity defect of both K261 and K364 (data not shown). Comparison of the complete sequence of this 4.3-kb fragment (GenBank accession number AF119670) with the *PTH11* cDNA sequence indicated that *PTH11* was the only ORF in this region (Figure 2A). Finally, we constructed gene disruption vectors (pCB1400 and pCB1401) that replaced the region between unique SpeI and KpnI sites in the *PTH11* ORF (Figure 2A) with the *HPH* gene. When we used these to disrupt the *PTH11* locus of strain 4091-5-8 by homologous recombination, the transformants exhibited pathogenicity defects indistinguishable from the original K261 and K364 *pth11* mutants (data not shown).

PTH11 is predicted to encode a protein of 631 amino acids (Pth11p) and is interrupted by six introns (Figure 2B). All of the intron splice junctions conformed to the GT–AG rule, and the lariat sites in introns 1 through 5 matched the consensus sequence RCTRAC. The lariat site in intron 6 (GCTAAA) was somewhat unusual (Figure 2B). Pth11p lacks significant similarity with any known protein. Hydropathy analysis of Pth11p with the TMpred program (Hofmann and Stoffel, 1993) predicts nine membrane insertion domains followed by a 269–amino acid hydrophilic domain (Figure 2C).

Impaired Appressorium Differentiation in *pth11* Mutants

To test whether *PTH11* is a pathogenicity-specific gene, we compared the vegetative growth and fertility of the *pth11* mutants K261 and K364 with wild-type strain 4091-5-8. In radial growth assays on oatmeal agar medium, the *pth11* mutants were identical to 4091-5-8 with respect to their growth rate, pigmentation, and ability to conidiate (data not shown). In addition, *pth11* mutants did not have an easily wettable phenotype, as has been described for mutants lacking the *MPG1* hydrophobin-encoding gene (Talbot et al., 1996). *M. grisea* is a heterothallic ascomycete. To determine the fertility of *pth11* mutants, we assayed the mating proficiency of strains K261 and K364 (both *MAT1-2*) when crossed with the near-isogenic wild-type strain 4454-R-1 (*MAT1-1*). Both mutants formed perithecia as efficiently as did the wild type, indicating that *PTH11* is not required for female fertility. In addition, when we crossed K261 and K364 with strain 4136-4-3 to monitor cosegregation of the *pth11* mutant phenotype with the *HPH* marker, we did not observe a reduction in ascospore viability associated with disruption of *PTH11*. Based on these observations, we concluded that *pth11* mutations specifically disrupt the *M. grisea* disease cycle but do not affect any other phase of the life cycle.

To determine the role of Pth11p in the disease cycle, we compared appressorium differentiation, penetration, invasive growth, and in-the-plant conidiation in wild-type and *pth11* mutant strains. To examine appressorium differentiation, we performed appressorium assays with the surface of barley leaves. Wild-type strain 4091-5-8 formed symmetrical, melanized appressoria at a frequency near 100% after 16 hr (Figure 4A and Table 1). In contrast, the *pth11* mutants K261 and K364 were severely impaired in their ability to produce appressoria (Figure 4B, Table 1, and data not shown). This impairment was not due to delayed differentiation, because upon prolonged incubation (24 hr), germ tubes continued to elongate without differentiating (Figure 4B).

Although appressorium formation was compromised in *pth11* mutants, we made two observations that suggest that differentiation was not completely incapacitated. First, *pth11* mutants continued to undergo germ tube hooking and apical swelling (Figure 4B), indicators of the early "recognition phase" of appressorium differentiation. Germ tube hooking and apical enlargement are infection-specific events and do not occur in undifferentiated vegetative hyphae produced on nutrient agar (Figures 4E and 4F). Second, *pth11* mutants formed morphologically normal appressoria at a frequency of 10 to 15% (Figure 4B and Table 1). These results suggest that Pth11p is important for completion of appressorium morphogenesis after the recognition phase of differentiation and that overlapping or parallel pathways may support differentiation at a reduced efficiency in *pth11* mutants.

Next, we tested whether the infrequent appressoria formed by *pth11* mutants were able to penetrate the leaf surface and form intracellular infection hyphae. To conduct this test, we used aniline blue epifluorescence to visualize penetration sites and intracellular hyphae. As shown in Figures 5A and 5B, appressoria formed by the *pth11* mutant K261 were able to penetrate and ramify as well as those of the wild-type strain 4091-5-8. As a further test for invasive growth, we inoculated mycelia from wild-type and *pth11* mutant strains over wound sites formed by puncturing barley leaves with an 18-gauge syringe needle. This allows for invasive growth that is independent of appressorium formation by direct entry of mycelia through the wound site. We found that the *pth11* mutants K261 and K364 were able to invade the wounded tissue as well as 4091-5-8 (data not shown). These results indicate that *PTH11* is not required for penetration or invasive growth.

By using aniline blue epifluorescence, we found that the wild-type strain 4091-5-8 formed multiple penetration sites in close proximity, whereas the *pth11* mutant formed penetration sites that were widely dispersed over the inoculation site due to the reduced frequency of appressorium differentiation (Figure 5). This may account for the observation that the virulence of *pth11* mutants was $<$1% of the wild type, yet appressorium formation was 10 to 15% of wild-type frequencies. If macroscopic lesions only form when there is an adequate coalescence of penetration sites, then most appressoria produced by *pth11* mutants would fail to yield lesions because they are well isolated. Fungal pathogens of plants often require multiple points of infection to form disease lesions, and it is thought that penetration sites in close proximity act synergistically to promote infection (Van der Plank, 1975).

Although the *pth11* mutants K261 and K364 conidiated as well as did the wild type on oatmeal agar medium, we were interested in determining whether they also conidiated efficiently in the plant. We previously found that mutations in the novel *PTH10* gene specifically abolished conidiation in culture but not in the plant (Sweigard et al., 1998). This suggests that distinct mechanisms govern conidiation during vegetative and pathogenic phases of the *M. grisea* life cycle. To determine whether *PTH11* was required for conidiation in the plant, we examined the surface of type 2 leaf lesions produced by wild-type and *pth11* mutant strains. Macroscopically, the lesions produced by wild-type and *pth11* mutant strains were velvety gray, and under a dissecting microscope, the conidial densities were similar. Thus, *PTH11* is not required for in-the-plant conidiation.

Localization of GFP-Tagged Pth11p

The predicted secondary structure of Pth11p suggested that it is an integral membrane protein (Figure 2C). To test whether Pth11p localizes to the cell membrane, we constructed a Pth11–GFP fusion protein and determined its intracellular distribution by using confocal laser scanning fluorescence microscopy. RNA gel blot analysis indicated that *PTH11* mRNA accumulated to barely detectable levels in both veg-

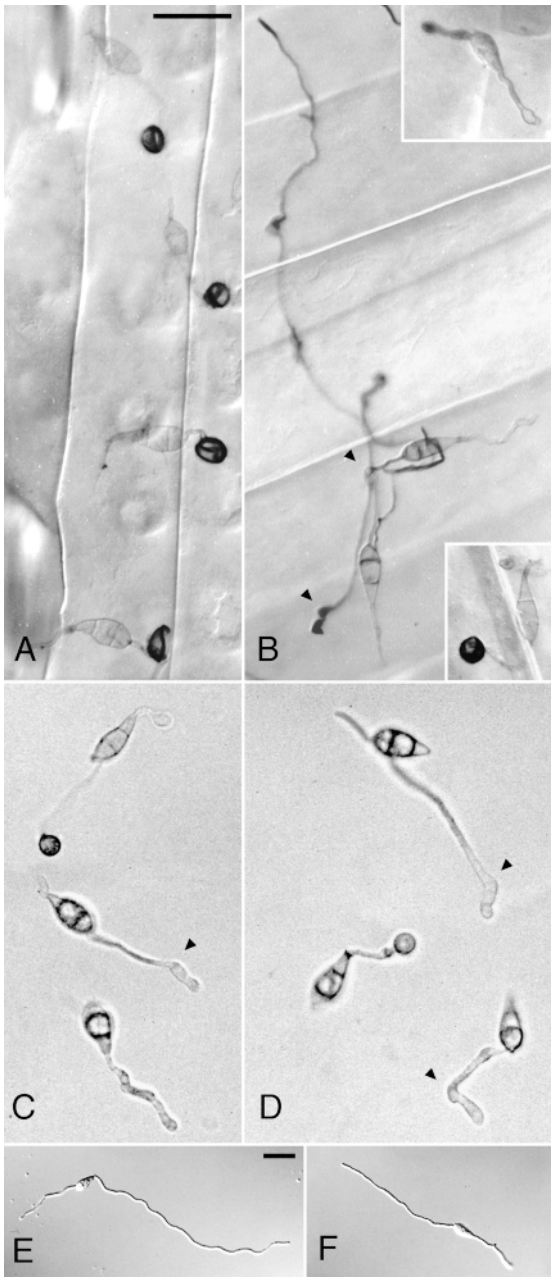

Figure 4. Germling Phenotypes of Wild-Type and *pth11* Mutant Strains.

Conidia were harvested from oatmeal agar plates for inoculation. Variations in appearance of these differential interference contrast images reflect optical abberations caused by sample preparation and/or substrates. Images of all germlings were recorded after 16 hr of incubation, except for the main image in **(B)**, which shows 24-hr germlings. The arrowheads indicate germ tube hooking; **(B)** shows a germ tube that hooked twice during a 24-hr incubation period but failed to form an appressorium. Results identical to those of strain K261 were observed with the *pth11* mutant K364.

(A) and **(B)** Wild-type **(A)** and *pth11* mutant **(B)** conidia resuspended in water and inoculated on excised barley leaves (cv Bonanza). The inoculated leaves were prepared as described in Methods. The collapsed appearance of some appressoria on the leaf surface is an artifact of the fixation procedure. The upper inset in **(B)** shows a typical *pth11* mutant germling with an enlarged apex, and the lower inset in **(B)** shows an infrequent *pth11* mutant germling that formed a morphologically normal appressorium.

(C) and **(D)** Wild-type **(C)** and *pth11* mutant **(D)** conidia resuspended in water and inoculated on the hydrophilic side of GelBond.

(E) and **(F)** Wild-type **(E)** and *pth11* mutant **(F)** conidia resuspended in complete medium and inoculated on microscope slides covered with complete medium plus 2% agarose.

Bar in **(A)** = 25 μm for **(A)** to **(D)**; bar in **(E)** = 25 μm for **(E)** and **(F)**.

etative and pathogenic germlings (data not shown). To facilitate detection of Pth11–GFP, we constructed gene fusions under the control of both the native *PTH11* promoter (pSM131) and the promoter of the gene encoding the *M. grisea* P2 ribosomal protein (pSM151). We previously found that the *P2* promoter mediates very high levels of gene expression during all stages of the *M. grisea* life cycle (A.M. Carroll and J.A. Sweigard, unpublished data). We transformed both of these *PTH11–GFP* fusion constructs into strain K261 and confirmed their presence by polymerase chain reaction and complementation of the phenotype of the *pth11* mutant (data not shown). For a negative control, we transformed K261 with a plasmid carrying Pth11p fused to the FLAG epitope (Pth11–FLAG) (pSM111). The FLAG fusion was at the same position in Pth11p as the GFP fusion. Pth11–FLAG was expressed from the *PTH11* promoter and complemented the *pth11* mutation (data not shown). For a positive control, we transformed the wild-type strain 4091-5-8 with a plasmid carrying *GFP* under the control of the *P2* promoter (pSM141).

For Pth11–GFP localization, we resuspended condia in defined complex medium containing 2 μg/mL 1,16-hexadecanediol and inoculated them onto the surface of a chambered coverglass. 1,16-Hexadecanediol is a plant cutin monomer that induces appressorium differentiation in *M. grisea* (Gilbert et al., 1996). Under these conditions, conidia formed appressoria at a frequency >90% and then grew vegetatively across the coverglass surface (see Methods). The majority of appressoria formed during the first 6 hr of incubation, but we were unable to detect Pth11–GFP fluorescence during this time. This did not appear to be due to a lack of gene expression, because overexpression of GFP from the *P2* promoter resulted in intense fluorescence during the first 6 hr of germination, whereas three independent K261 transformants and a 4091-5-8 transformant that overexpressed Pth11–GFP from the *P2* promoter did not fluoresce (data not shown).

Vegetative hyphae emerged between 6 and 24 hr after inoculation. In vegetative hyphae overexpressing Pth11–GFP, we observed increased fluorescence at the cell periphery

Table 1. Effects of cAMP and Diacylglycerol on Appressorium Formation and Pathogenicity

Strain	*PTH11*	Inoculation Conditions[a]	% Appressoria[b] (Leaf)[c]	% Appressoria (GelBond)[d]	Pathogenicity[e]
4091-5-8	+	H_2O	97 ± 3.2	2.3 ± 2.1	5
4091-5-8	+	cAMP	93 ± 3.6	ND[f]	5
4091-5-8	+	DAG	100 ± 0.58	ND	5
K261	−	H_2O	10 ± 5.9	1.7 ± 2.1	Rare 2
K261	−	cAMP	82 ± 20	ND	5
K261	−	DAG	51 ± 26	ND	Rare 2
K364	−	H_2O	11 ± 2.7	ND	Rare 2
K364	−	cAMP	71 ± 25	ND	5
K364	−	DAG	63 ± 15	ND	Rare 2

[a] cAMP was used at a final concentration of 10 mM and the diacylglycerol (DAG) 1,2-dioctanoylglycerol-*rac*-glycerol was used at a final concentration of 20 μg/mL.

[b] Appressorium assays were scored 16 to 20 hr after inoculation. Values are the mean ±SD of three independent assays in which ⩾100 germlings were scored.

[c] The barley cultivar Bonanza was used for leaf assays.

[d] GelBond refers to the hydrophilic side of GelBond (agarose-coated polyester).

[e] Dominant lesion type formed in a standard infection assay on barley (cv Bonanza).

[f] ND, not determined.

and intense fluorescence in internal compartments throughout the germling (Figure 6B). We concluded that these internal compartments were vacuoles because the fluorescent signal overlaid the vacuoles, as defined by depressions seen in the corresponding differential interference contrast image (Figure 6A). Localization of Pth11–GFP to the vacuole was not due to fusion to GFP because GFP is excluded from the vacuole (Figures 6G and 6H). Furthermore, the vacuolar localization was not due to overexpression of Pth11–GFP from the *P2* promoter because Pth11–GFP expressed from the *PTH11* promoter also localized to the vacuole, although the intensity of fluorescence was greatly reduced (Figures 6C and 6D). As with the overexpressed protein, Pth11–GFP expressed from the native promoter was visible only after appressorium differentiation was complete. We were unable to detect native levels of Pth11–GFP at the cell membrane at any time. Cell surface and vacuolar fluorescence was not detectable in cells expressing the Pth11–FLAG fusion protein, indicating that the fluorescence was specific to the Pth11–GFP fusion protein (Figures 6E and 6F). We conclude that Pth11p is a membrane protein that may be endocytosed and targeted to the vacuole.

Surface Sensing Defect of *pth11* Mutants

Appressorium differentiation in *M. grisea* is induced by soluble plant cutin monomers and contact surface hydrophobicity. Surfaces lacking these inductive cues, such as the hydrophilic side of GelBond (agarose-coated polyester), fail to support efficient differentiation of appressoria. The phenotype of wild-type strain 4091-5-8 on the hydrophilic side of GelBond is reminiscent of *pth11* mutants on the leaf surface (Figure 4C). The germlings undergo the early stages of appressorium differentiation, as evidenced by germ tube hooking and apical swelling, but mature appressoria rarely form. Also, those appressoria that do form are morphologically normal. Thus, failure to detect inductive substrate cues results in impaired appressorium maturation after germ tube hooking and apical swelling. The formation of germ tube hooks and apical enlargements by 4091-5-8 on the hydrophilic side of GelBond is not dependent on the function of Pth11p, because the *pth11* mutant K261 also forms these structures when germinated on this surface (Figure 4D). Based on these results, we hypothesize that inductive substrate cues activate appressorium maturation via Pth11p subsequent to germ tube hooking and apical swelling.

To determine whether *pth11* mutants responded specifically to either cutin monomers or contact surface hydrophobicity, we performed in vitro appressorium assays in the presence and absence of these inducers. The *pth11* mutant K261 formed appressoria at a frequency of 15% on polystyrene, a neutral surface, and 12% on polystyrene supplemented with 1,16-hexadecanediol. K261 formed appressoria at a frequency of 10% on Teflon, a hydrophobic surface, and 8% on Teflon supplemented with 1,16-hexadecanediol. Thus, in each of these in vitro assays, K261 formed appressoria at a frequency similar to that observed in the plant (Table 1). In contrast to K261, wild-type strain 4091-5-8 formed appressoria at a frequency of 11% on polystyrene and 94% on polystyrene supplemented with 1,16-hexadecanediol. 4091-5-8 formed appressoria at a frequency of 96% on Teflon and 98% on Teflon supplemented with 1,16-hexadecanediol. These results indicate that cutin monomers and contact surface hydrophobicity activate appressorium differentiation in strain 4091-5-8 and that Pth11p is required for efficient appressorium formation in response to both of these inductive cues.

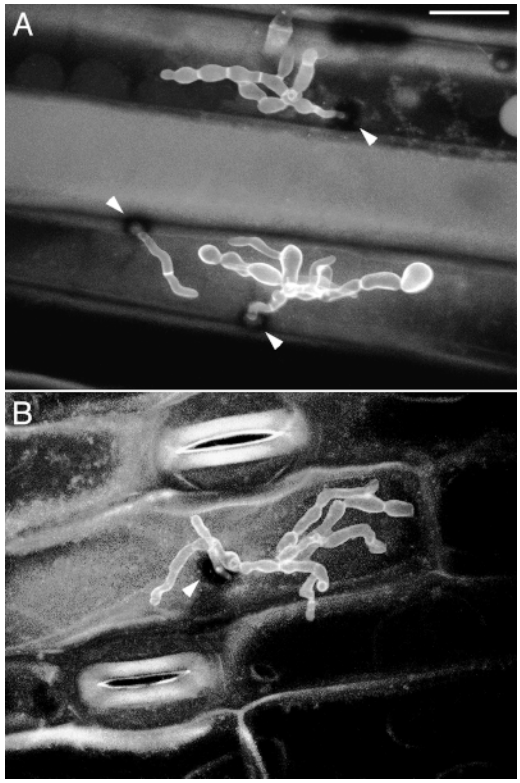

Figure 5. Visualization of Infection Hyphae in Wild-Type and *pth11* Mutant Strains.

Conidia were inoculated on excised barley leaves (cv BarSoy), incubated at 23°C for 112 hr, and stained with aniline blue. The images are maximum intensity projections of a z-series of optical sections taken with a laser scanning confocal microscope. The arrowheads indicate the location of appressoria on the leaf surface.

(A) Wild-type strain 4091-5-8. The distribution of the three penetration sites shown is representative of the entire field of inoculation.

(B) *pth11* mutant strain K261. The single penetration site shown is well isolated due to the reduced frequency of appressorium differentiation in this strain.

Bar in **(A)** = 25 μm for **(A)** and **(B)**.

Although the phenotype of wild-type strain 4091-5-8 on the hydrophilc side of GelBond was similar to that of *pth11* mutants on the leaf surface, we found that 4091-5-8 formed appressoria at a significantly lower frequency on the hydrophilic side of GelBond than did the *pth11* mutant K261 on the leaf surface (applying Student's *t* test; $t = 2.23$; $P < 0.05$; degrees of freedom [df] = 4) (Table 1). Furthermore, when we compared the appressorium frequency of K261 on the hydrophilic side of GelBond with that of K261 on the leaf surface, we also observed a significantly lower frequency of appressoria on the hydrophilic side of GelBond ($t = 2.48$; $P < 0.05$; df = 4) (Table 1). However, we did not observe a significant difference in the appressorium frequencies of the wild-type strain 4091-5-8 and the *pth11* mutant K261 when both were germinated on the hydrophilic side of GelBond ($t = 0.447$; $P > 0.10$; df = 4). These results are consistent with a model in which multiple signaling pathways functionally overlap to activate appressorium morphogenesis. The observation that both wild-type and *pth11* mutant germlings form appressoria at a lower frequency on the hydrophilic side of GelBond suggests that Pth11p-mediated signaling and functionally overlapping pathways are downregulated in the absence of inductive cues.

Pharmacological Suppression of *pth11* Mutant Phenotypes

Appressorium differentiation in *M. grisea* is the result of coordinated input from multiple cellular signaling pathways, including multiple cAMP-mediated pathways and, possibly, a diacylglycerol-mediated pathway (Lee and Dean, 1993; Thines et al., 1997; Adachi and Hamer, 1998). We hypothesized that Pth11p acts at the plasma membrane to mediate appressorium differentiation in response to inductive substrate cues by playing an upstream signaling role in one or more of these pathways. To test whether Pth11p plays an upstream signaling role, we exogenously activated cAMP- and diacylglycerol-mediated signaling in wild-type strain 4091-5-8 and the *pth11* mutants K261 and K364 and examined their ability to form appressoria and cause disease (Table 1 and Figure 7).

In leaf appressorium assays, the wild-type strain formed appressoria at a frequency >90%, regardless of drug treatment (Table 1). In contrast, *pth11* mutants exhibited impaired appressorium differentiation in the absence of drug treatment, and both cAMP and diacylglycerol suppressed this defect (Table 1). Treatment of K261 and K364 with cAMP appeared to suppress the appressorium defect better than diacylglycerol, and when we treated *pth11* mutants with both drugs, we observed levels of appressoria similar to treatment with cAMP alone (data not shown). Appressoria formed by *pth11* mutants after treatment with cAMP or diacylglycerol were indistinguishable from appressoria formed by the wild-type strain. Thus, exogenous activation of cAMP- or diacylglycerol-mediated signaling suppressed the appressorium defect of the *pth11* mutants K261 and K364.

Although cAMP and diacylglycerol suppressed the appressorium defect of *pth11* mutants, the ability to form appressoria is not sufficient for pathogenicity. For example, mutations in the mitogen-activated protein kinase homolog *MPS1* do not affect appressorium formation but abolish pathogenicity by preventing penetration through the host surface (Xu et al., 1998). To determine whether exogenous cAMP and diacylglycerol also suppressed the pathogenicity defect of *pth11* mutants, we performed pathogenicity assays with barley seedlings in the presence of these compounds (Figure 7 and Table 1). cAMP and diacylglycerol, either alone or in combination, did not affect the

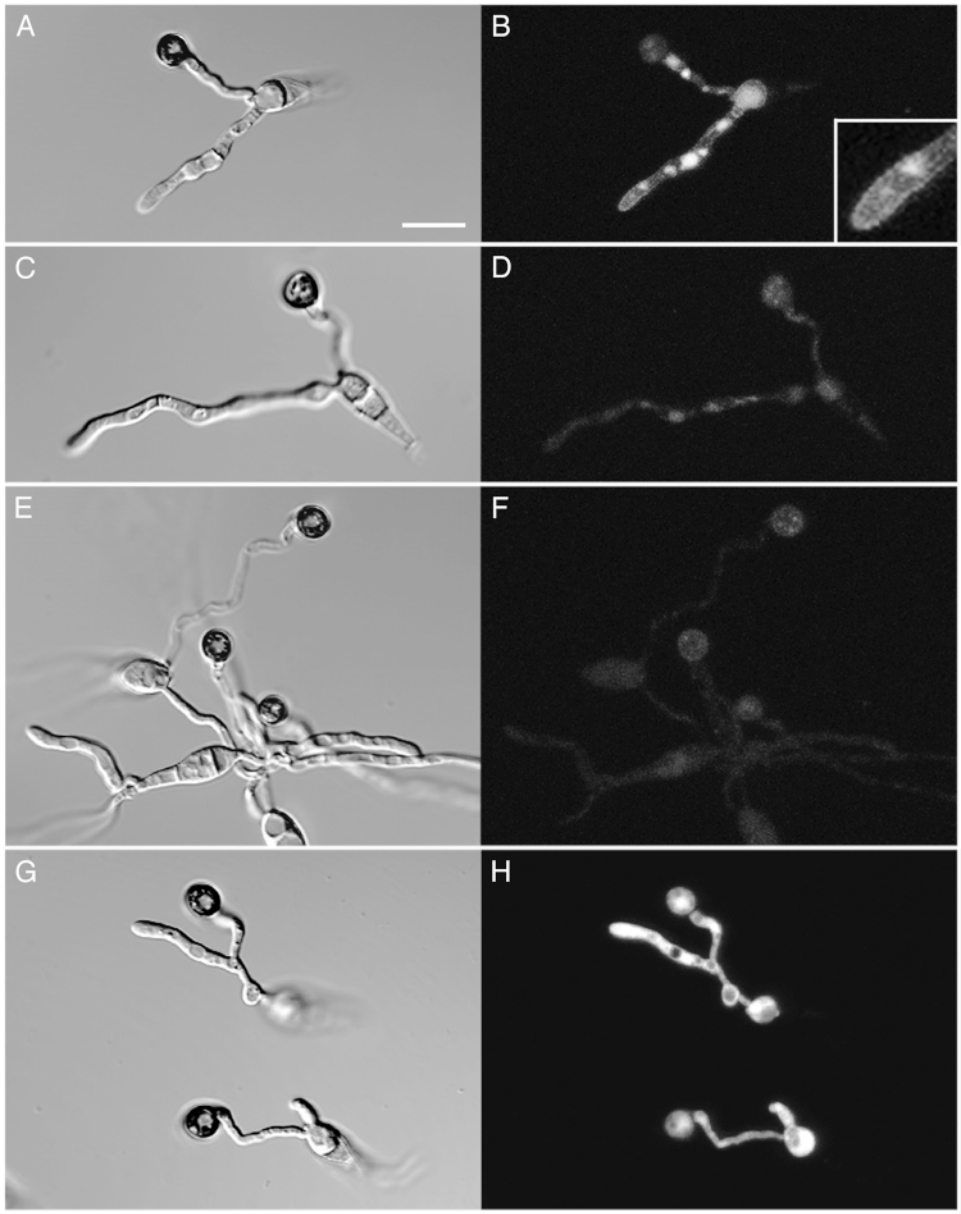

Figure 6. Imaging of Pth11–GFP.

Conidia were resuspended in defined complex medium containing 2 μg/mL 1,16-hexadecanediol and inoculated on a coverglass surface. Differential interference contrast and corresponding GFP fluorescence images were recorded after 24 hr. Images of GFP fluorescence represent a maximum intensity projection of a z-series of optical sections taken with a laser scanning confocal microscope. The inset in **(B)** is enlarged 200% to facilitate visualization of cortical fluorescence.
(A) and **(B)** K261 expressing *PTH11–GFP* from the *P2* promoter (strain MG73).
(C) and **(D)** K261 expressing *PTH11–GFP* from the *PTH11* promoter (strain MG19).
(E) and **(F)** K261 expressing *PTH11–FLAG* from the *PTH11* promoter (strain CP4445).
(G) and **(H)** 4091-5-8 expressing *GFP* from the *P2* promoter (strain CP4346).
Bar in **(A)** = 12.5 μm for **(A)** to **(H)**.

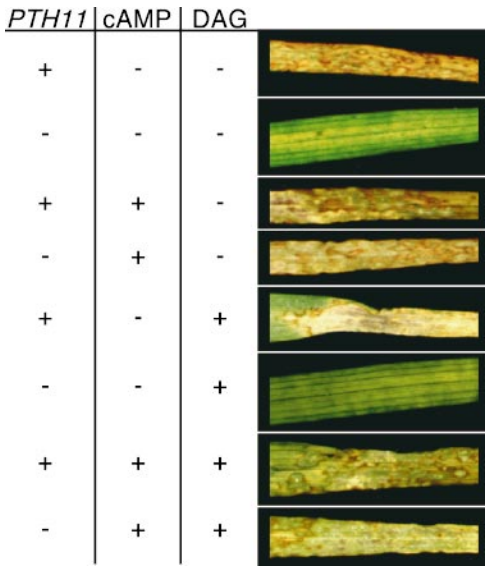

Figure 7. Effects of Exogenous cAMP and Diacylglycerol on Pathogenicity.

Barley plants were spray inoculated with conidial suspensions of wild-type strain 4091-5-8 (+) and *pth11* mutant strain K261 (−) and supplemented with 10 mM cAMP or 20 μg/mL diacylglycerol (DAG), where indicated. Representative leaves were collected 5 days after inoculation and photographed.

pathogenicity of wild-type strain 4091-5-8, and severe type 5 disease lesions formed in each case. In contrast, the *pth11* mutant K261 was nonpathogenic in the absence of cAMP or diacylglycerol. The pathogenicity defect of K261 was suppressed by cAMP, resulting in severe type 5 disease lesions similar to those formed by strain 4091-5-8. Although diacylglycerol suppressed the appressorium defect of the *pth11* mutants, we did not observe any effect of diacylglycerol on the pathogenicity defect of K261. Finally, the addition of both cAMP and diacylglycerol to K261 yielded results similar to cAMP alone. These experiments were performed simultaneously with the *pth11* mutant K364, and identical results were observed (data not shown).

These results suggest that Pth11p is an upstream activator of either cAMP-mediated signaling or a functionally overlapping signaling pathway. Because diacylglycerol suppressed the appressorium defect of *pth11* mutants, it also appears to play a signaling role in *M. grisea*. However, diacylglycerol-mediated signaling does not appear to be sufficient for pathogenicity. An alternative explanation for our results with exogenous diacylglycerol is that this compound mimics the inductive effects of plant cutin monomers. This is unlikely because cutin monomers fail to induce appressorium differentiation in *pth11* mutants. In addition, although both diacylglycerol and 1,16-hexadecanediol contain fatty acid chains, their structures are otherwise dissimilar, and a stringent structure–activity relationship has been established for cutin monomer–like compounds that induce appressorium differentiation in *M. grisea* (Gilbert et al., 1996).

Plasticity of Pth11p Function among Related *M. grisea* Strains

M. grisea is a complex fungal species capable of infecting many different species of grass. However, individual *M. grisea* strains have a relatively narrow host range and are capable of infecting only one or a few grass species (Ou, 1985; Valent, 1997). *M. grisea* strains with similar host specificities are closely related, and molecular analysis of mitochondrial DNA sequence polymorphisms has been used to identify host-specific haplotypes (Valent, 1997; A.R. Kubelik, J.A. Sweigard, F.G. Chumley, and B. Valent, unpublished data). We recovered the *pth11* mutants K261 and K364 from an insertional mutagenesis screen with the barley pathogen 4091-5-8, a mitochondrial DNA haplotype I laboratory strain. Because all rice pathogens that have been identified also belong to mitochondrial DNA haplotype I, we were interested in characterizing the function of Pth11p in other members of this haplotype. We introduced *pth11* null mutations into the rice pathogens 6043, 4224-7-8, Guy11, and CP987 by homologous recombination. We then scored the following phenotypes of these strains: appressorium formation on the leaf surface, appressorium formation on the hydrophilic side of GelBond, and pathogenicity in plant infection assays (Table 2).

As with strain 4091-5-8, strains 6043, 4224-7-8, Guy11, and CP987 were pathogenic in plant infection assays and formed appressoria at a frequency near 100% on the leaf surface. However, these strains varied in their ability to differentiate on the hydrophilic side of GelBond. Strain 6043 was similar to strain 4091-5-8 and formed few appressoria on this surface, strains 4224-7-8 and Guy11 formed appressoria at a slightly higher frequency than 4091-5-8 and 6043, and CP987 formed appressoria at the same frequency on the hydrophilic side of GelBond as it did on the leaf surface. Based on these results with CP987, we believe that this strain may have acquired a mutation during its construction that causes constitutive activation of appressorium differentiation. Consistent with the hypothesis that CP987 is constitutively activated for appressorium differentiation, this strain forms appressoria in the presence of yeast extract, whereas yeast extract inhibits appressorium formation in the CP987 parent, strain 4360-17-1 (P. Bobrowicz and D. Ebbole, personal communication). The inhibitory effects of yeast extract have previously been shown to be suppressed by constitutive activation of appressorium differentiation with exogenous cAMP (Beckerman and Ebbole, 1996).

We observed a number of differences in the phenotypes of the *pth11* mutants of strains 6043, 4224-7-8, Guy11, and CP987. *PTH11* was essential for pathogenicity and efficient appressorium differentiation on the leaf surface in strains 6043 and Guy11 but not 4224-7-8 and CP987. On the

Table 2. Effect of *pth11* Mutations on Rice Pathogens[a]

Strain	*PTH11*	% Appressoria[b] (Leaf)[c]	% Appressoria (GelBond)[d]	Pathogenicity[e]
6043	+	97 ± 3.6	2.3 ± 1.5	5
CP4124	−	9.7 ± 7.1	2.3 ± 0.58	Rare 2
4224-7-8	+	96 ± 3.6	11 ± 4.0	3-4
CP4116	−	93 ± 7.2	96 ± 0.58	1-2
Guy11	+	96 ± 0.58	8.7 ± 3.2	5
CP3385	−	18 ± 3.1	54 ± 3.2	Rare 2
CP987	+	96 ± 1.1	97 ± 2.3	5
CP3368	−	78 ± 21	66 ± 20	5

[a] Each strain belongs to mitochondrial DNA haplotype I and infects rice and barley. Three independent *pth11* mutants of each parent strain were tested and yielded similar results.

[b] Appressorium assays were scored 16 to 20 hr after inoculation. Values are the mean ±SD of three independent assays in which ⩾100 germlings were scored.

[c] Barley cultivar Bonanza or BarSoy was used for leaf assays and yielded identical results.

[d] GelBond refers to the hydrophilic side of GelBond (agarose-coated polyester).

[e] Dominant lesion type formed in standard infection assays. Assays were performed on multiple hosts; the values shown are from assays on the most susceptible host. 6043/CP4124 were assayed on barley cultivar Bonanza; Guy11/CP3385 and CP987/CP3368 were assayed on rice cultivar Sariceltic; and 4224-7-8/CP4116 were assayed on rice cultivar CO39.

hydrophilic side of GelBond, the 6043 *pth11* mutant formed appressoria at a very low frequency, similar to the 4091-5-8 *pth11* mutants. In contrast, the *pth11* mutants of strains 4224-7-8, Guy11, and CP987 formed appressoria at a high frequency on the hydrophilic side of GelBond. Because the *pth11* mutant of CP987 may be constitutively activated for differentiation downstream from Pth11p, we excluded this strain from further analysis and drew the following conclusions from the remaining data. First, our observation that *pth11* mutants of 4224-7-8 and Guy11 form appressoria at a high frequency indicates that multiple pathways mediate differentiation and that the relative contribution of these pathways to differentiation varies among *M. grisea* strains. Second, these data implicate Pth11p as a repressor of appressorium differentiation on poorly inductive surfaces in strain 4224-7-8 because the *pth11* mutant of this strain forms appressoria efficiently on the hydrophilic side of GelBond, whereas the wild-type parent does not. Finally, because the *pth11* mutant of Guy11 is deficient for appressorium differentiation on the leaf surface but forms appressoria at a high level on the hydrophilic side of GelBond, Pth11p both activates appressorium differentiation in response to inductive substrate cues and represses differentiation on poorly inductive substrates in strain Guy11.

Conservation of Pth11p Function among Diverse *M. grisea* Strains

To determine whether Pth11p function was conserved in *M. grisea* strains outside of mitochondrial DNA haplotype I, we tested *PTH11* genes from diverged *M. grisea* strains for functionality in wild-type strain 4091-5-8. We identified *PTH11* in *M. grisea* strains that infect a wide range of grass hosts by DNA gel blot hybridization analysis, using the *PTH11* cDNA from pCB1312 as a probe. *PTH11* was conserved in every strain, including those with significantly divergent mtDNA haplotypes (data not shown). *M. grisea* strains G-11 and G-207 demonstrated reduced hybridization to the *PTH11* cDNA probe, suggesting that sequence variations occurred in these two isolates. G-11 belongs to haplotype IIa and G-207 belongs to haplotype III. To examine the sequence of *PTH11* from strains G-11 and G-207, we constructed λ phage genomic DNA libraries of these two strains (see Methods) and isolated *PTH11* genomic clones (pSM79 and pSM85) by hybridization with the *PTH11* cDNA probe. We then sequenced the G-11 and G-207 *PTH11* genes (GenBank accession numbers AF119671 and AF119672, respectively). Figure 8 shows an alignment of the predicted Pth11p amino acid sequences from 4091-5-8, G-11, and G-207. Pth11p from 4091-5-8 was 87% identical to Pth11p from G-11 and 86% identical to Pth11p from G-207, whereas the G-11/G-207 identity was 87.4%. To test functional conservation of these *PTH11* genes, we transformed K261 with the G-11 and G-207 *PTH11* genomic clones. Both *PTH11* genes were capable of complementing the appressorium and pathogenicity defects of the *pth11* mutant K261 (data not shown) (see Table 3, CP4329 and CP4336). Thus, the G-11 and G-207 *PTH11* isoforms can functionally substitute for *PTH11* in strain 4091-5-8, indicating that Pth11p is highly conserved throughout the *M. grisea* species.

DISCUSSION

Considerable progress has been made in elucidating signaling components that govern appressorium formation in *M.*

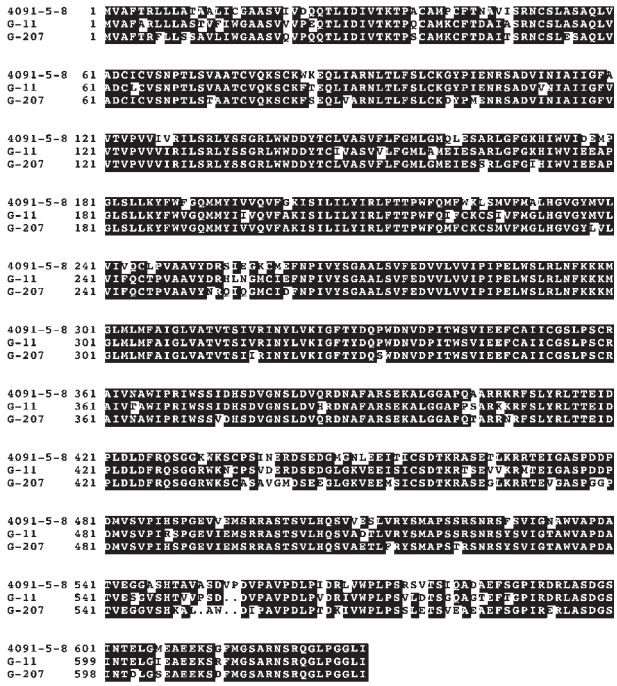

Figure 8. Amino Acid Alignment of Pth11p from Distantly Related *M. grisea* Strains.

The predicted Pth11p sequences from *M. grisea* strains 4091-5-8, G-11, and G-207 were aligned using the PILEUP program from the Genetics Computer Group's software package and processed with the MacBoxshade 2.11 program (shareware available at ftp://ulrec3.unil.ch/pub/boxshade/macboxshade). Black-boxed residues indicate amino acid identities.

grisea: a prototypical G protein/adenylate cyclase/cAMP–dependent protein kinase A activating circuit functions simultaneously with multiple mitogen-activated protein kinase cascades to ensure rapid differentiation and penetration of host tissue (Mitchell and Dean, 1995; Xu and Hamer, 1996; Choi and Dean, 1997; Liu and Dean, 1997; Xu et al., 1997, 1998; Adachi and Hamer, 1998). However, the initial events of substrate sensing and transduction of extracellular cues into an intracellular signal are poorly understood. Analysis of nonpathogenic insertional mutants of *M. grisea* strain 4091-5-8 revealed a novel transmembrane protein-encoding gene, *PTH11*, that governs appressorium differentiation in response to inductive substrate cues.

Model for Pth11p Function in *M. grisea* Strain 4091-5-8

PTH11 is a pathogenicity gene in the strictest sense of the term (Schafer, 1994) because *pth11* mutations specifically affect pathogenicity but no other phase of the *M. grisea* life cycle. *pth11* mutants of *M. grisea* strain 4091-5-8 fail to differentiate beyond the early recognition phase of appressorium formation. This is not due to a defect in appressorium structure or function, because the occasional appressoria formed by *pth11* mutants have a wild-type morphology and penetrate and ramify throughout host tissue as efficiently as do those of the wild type. Rather, the phenotype of *pth11* mutants on the host surface is similar to that of wild-type *M. grisea* strains on a poorly inductive surface. In both cases, germ tube hooking and apical swelling occur, but mature appressoria form at a greatly reduced frequency. Germ tube hooking and apical swelling appear to reflect a critical recognition phase in which the fungus commits either to terminal differentiation of an appressorium or to further germ tube growth across the substratum (Bourett and Howard, 1990). Our data indicate that Pth11p plays an important role in the commitment to appressorium differentiation during this phase.

Hydropathy analysis of Pth11p predicts an integral membrane protein with multiple membrane-spanning regions. Consistent with this, we localized a Pth11–GFP fusion to the cell cortex; however, the protein was predominantly associated with internal compartments, especially vacuoles. This pattern of localization is similar to that of mating pheromone receptors and membrane transporters in *Saccharomyces cerevisiae* (reviewed in Hicke, 1999). In *S. cerevisiae*, the activity of these proteins is modulated by the amount of protein at the membrane. Endocytosis and degradation in the vacuole quickly reduce protein levels. For receptors, this rapid downregulation allows the cell to return to a basal state after signal activation and cellular response. Our results suggest that Pth11p levels may be regulated in this manner because Pth11–GFP was only visible in vacuoles after appressorium differentiation, when downregulation is predicted.

Exogenous cellular second messengers suppressed defects associated with *pth11* mutants, suggesting that Pth11p mediates appressorium differentiation by activating intracellular signaling. cAMP appeared to be the most physiologically relevant second messenger tested because it suppressed the appressorium defect of *pth11* mutants and restored wild-type levels of pathogenicity. It is unclear whether diacylglycerol is an activator of protein kinase C in fungi as it is in other eukaryotes (Antonsson et al., 1994; Watanabe et al., 1994), but the ability of diacylglycerol to suppress the appressorium defect of *pth11* mutants suggests a signaling role for this compound in *M. grisea*. Two possible explanations for the inability of diacylglycerol to restore the pathogenicity of *pth11* mutants are that it fortuitously activates appressorium differentiation in a way that is not physiologically relevant or that diacylglycerol-mediated signaling alone is insufficient to cause disease but may contribute to infection-specific differentiation by acting in conjunction with additional signaling pathways.

Although our data suggest that Pth11p acts at the cell surface as an effector of differentiation, the exact function of the protein is unknown. A plausible model for Pth11p in *M.*

Table 3. Fungal Strains Used in This Study[a]

Name	MT[b]	Description/Reference
4091-5-8	1-2	Valent et al. (1991)
4136-4-3	1-1	Valent and Chumley (1987)
4224-7-8	1-1	Sweigard et al. (1995)
4360-17-1	1-1	Progeny of a cross between 4224-7-8 and 6043
4454-R-1	1-1	Nearly isogenic to 4091-5-8; derived by extensive backcrossing of 4091-5-8 × 4136-4-3 *MAT1-1* progeny to 4091-5-8
6043	1-2	Leung et al. (1988)
G-11	ND[c]	Crabgrass pathogen; Japanese field isolate
G-207	ND	*Cenchrus echinatus* pathogen; Brazilian field isolate
Guy11	1-2	French Guyana field isolate (Leung et al., 1988)
K261	1-2	*pth11* mutant of 4091-5-8 constructed by KpnI REMI of pCB1004
K364	1-2	*pth11* mutant of 4091-5-8 constructed by KpnI REMI of pCB1004
CP987	1-1	*avr-pwl2 avr2-Pita* double mutant of 4360-17-1
CP3385	1-2	*pth11* mutant of Guy11 constructed by homologous recombination with pCB1400
CP3368	1-1	*pth11* mutant of CP987 constructed by homologous recombination with pCB1400
CP4116	1-1	*pth11* mutant of 4224-7-8 constructed by homologous recombination with pCB1400
CP4124	1-2	*pth11* mutant of 6043 constructed by homologous recombination with pCB1400
CP4154	1-2	K261 transformed and complemented with pCB1272
CP4329	1-2	K261 cotransformed and complemented with pCB1530 (Sweigard et al., 1997) and pSM79 (plasmid carrying G-11 *PTH11* homolog
CP4336	1-2	K261 cotransformed and complemented with pCB1530 (Sweigard et al., 1997) and pSM85 (plasmid carrying G-207 *PTH11* homolog
CP4346	1-2	4091-5-8 cotransformed with pCB1004 (Carroll et al., 1994) and pSM141
CP4445	1-2	K261 cotransformed and complemented with pCB1530 (Sweigard et al., 1997) and pSM111
MG19	1-2	K261 cotransformed and complemented with pCB1530 (Sweigard et al., 1997) and pSM131
MG73	1-2	K261 cotransformed and complemented with pCB1530 (Sweigard et al., 1997) and pSM151

[a] All strains belong to mitochondrial DNA haplotype I, except for G-11 (haplotype IIa) and G-207 (haplotype III).
[b] MT, mating type.
[c] ND, not determined.

grisea strain 4091-5-8 is that it is a receptor for inductive surface cues. Like Pth11p, many receptors have a high degree of functional specificity because they initiate complex morphological processes that culminate in a terminally differentiated state (Gudermann et al., 1996). However, eukaryotic serpentine receptors typically have seven transmembrane regions (Bockaert and Pin, 1999), whereas Pth11p appears to have nine; thus, either the hydropathy analysis is inaccurate or Pth11p is an atypical receptor. Also, if Pth11p is a receptor, then its activator is not immediately apparent, because *pth11* mutants demonstrate impaired response to both hydrophobicity and cutin monomers.

Pth11p in Multiple *M. grisea* Strains: Capriciousness in Protein Function

Our results with multiple *M. grisea* strains yielded a number of insights regarding Pth11p function and infection-specific signaling that we would not have otherwise discovered by studying a single strain. In strains 4091-5-8 and 6043, the phenotype of the *pth11* mutant was consistent with a role for Pth11p as an activator of appressorium differentiation, whereas in strain 4224-7-8, the phenotype suggested a role as a repressor of differentiation under noninductive conditions. In strain Guy11, the phenotype was intermediate and suggested a role for Pth11p as both an activator of differentiation on inductive surfaces and a repressor of differentiation on noninductive surfaces. Despite these apparent differences in function, we found that Pth11p homologs from very diverged *M. grisea* strains were highly conserved and fully complemented the 4091-5-8 *pth11* mutant. The mechanism of Pth11p-mediated repression of differentiation cannot be distinguished by our results; however, signaling is often modulated by specific receptor regulatory domains. For example, after activation by the α mating pheromone, the C terminus of the budding yeast α pheromone receptor is hyperphosphorylated, resulting in receptor desensitization and downregulation (Hicke et al., 1998). We are currently investigating whether the activating and repressing functions of Pth11p can also be assigned to specific protein domains.

Complexity of Infection-Related Signaling in *M. grisea*

We made two observations in support of the current model that proposes multiple effectors of appressorium differentiation. First, although 4091-5-8 *pth11* mutants are defective in

appressorium differentiation, they continue to respond to inductive substrate cues and form appressoria at a frequency of 10 to 15%. Second, *pth11* mutants of 4224-7-8 form appressoria at wild-type levels, suggesting a functional overlap between Pth11p and other activating factors in this strain. We have begun to analyze this functional overlap by crossing the *pth11* mutant of 4224-7-8 with the *pth11* mutant of 6043, finding that the Pth11p overlapping activity segregates as a single gene (data not shown).

Our analysis of Pth11p function in multiple *M. grisea* strains suggests a level of intricacy in the prevailing model of appressorium differentiation that has not previously been observed: closely related *M. grisea* strains deploy their signaling effectors in substantially different ways. We reject the hypothesis that Pth11p is a fundamentally distinct protein in the various strains tested, because protein structure and function are highly conserved in diverged *M. grisea* strains. Rather, we believe these results highlight the complexity of *M. grisea* as a species and suggest that plasticity in signaling may be an effective means of adaptation to host defense mechanisms and other environmental stress.

Although signal transduction is often conceived of as a linear event, our and previous studies indicate that infection-specific signaling in *M. grisea* is a complex, nonlinear process. In *M. grisea* strain 4091-5-8, we find that Pth11p is required for appressorium differentiation in response to both surface hydrophobicity and cutin monomers, yet these inducers are thought to be processed in parallel and converge on adenylate cyclase (Mac1p) (Choi and Dean, 1997). From Mac1p it has been proposed that the signal again diverges to yield multiple cAMP-dependent pathways that mediate different aspects of appressorium morphogenesis and function (Adachi and Hamer, 1998). In addition, at least two mitogen-activated protein kinase cascades, overlaid on these cAMP cascades, are also required for appressorium penetration and morphogenesis (Xu and Hamer, 1996; Xu et al., 1998). This model of appressorium differentiation in *M. grisea* conforms to the current view of cellular signaling as a complex network composed of divergent and convergent pathways at each transduction level (Gudermann et al., 1996).

METHODS

Fungal Strains, Culture, and Transformation

The *Magnaporthe grisea* strains used in this study are described in Table 3. All strains were cultured and stored as described by Valent et al. (1991). Transformation of *M. grisea* protoplasts was performed as described by Sweigard et al. (1995). Transformants were selected on either defined complex medium (0.17% yeast nitrogen base without amino acids and NH_4SO_4, 0.1% NH_4NO_3, 0.2% asparagine, 1% glucose, and 1.7% agar, pH 6.0, with Na_2HPO_4) containing 25 μg/mL Bialophos (gluphosinate ammonium; Crescent Chemical Co., Inc., Hauppage, NY) or complete medium (0.6% yeast extract, 0.6% casein hydrolysate, 1% glucose, and 1.7% agar) containing 200 μg/mL hygromycin B (Sigma). Transformation plates were incubated for 4 to 5 days at 23°C in the dark, after which primary transformants were transferred to oatmeal agar plates (Crawford et al., 1986) and purified by monoconidiation. Genetic crosses were performed as described by Valent et al. (1991).

Plasmids, DNA Libraries, and DNA Manipulations

The plasmids used in this study are described in Table 4. The cloning vectors pBC SK+ and pBluescript II SK− were acquired from Stratagene (La Jolla, CA). Genomic DNA libraries were constructed from strains 4091-5-8, G-11, or G-207 in λ Barfix (Sweigard et al., 1998) or λ NFSFix, a λ replacement vector derived from Barfix. A cDNA library was constructed from strain 6043 in the λ ZipLox vector (Gibco BRL), as described by Sweigard et al. (1998), using pooled poly(A)$^+$ mRNA from a variety of growth and differentiation conditions. DNA gel blot analysis was performed with Hybond-N transfer membranes (Amersham Pharmacia Biotechnology, Piscataway, NJ), according to Sambrook et al. (1989). Sequencing was performed on an ABI Prism automated sequencer (model 377; Perkin-Elmer, Norwalk, CT). Sequence analysis was performed using the Genetics Computer Group software package version 10.0 (Genetics Computer Group, Madison, WI). Pairwise comparisons of Pth11p sequences from *M. grisea* strains 4091-5-8, G-11, and G-207 were performed using the Genetics Computer Group BestFit program. All enzyme manipulations were performed according to manufacturer's protocols. Restriction enzymes and polymerase chain reaction reagents were acquired from Gibco BRL, and T4 DNA ligase was acquired from New England Biolabs (Beverly, MA). *Saccharomyces cerevisiae* W303-1a was used for construction of the *PTH11–green fluorescent protein* (*GFP*) gene fusion by gap repair homologous recombination (Oldenburg et al., 1997). Bidirectional sequencing to ensure fidelity followed all cloning strategies that involved polymerase chain reaction or homologous recombination in yeast.

Plant Infection Assays

Standard infection assays were performed with aerosolized conidia, as described previously (Sweigard et al., 1998), using barley (*Hordeum vulgare*) cultivars Bonanza and BarSoy, rice (*Oryza sativa*) cultivars Sariceltik and CO39, or weeping lovegrass (*Eragrostis curvula*). Briefly, 8- to 14-day-old conidia were harvested and resuspended in 0.25% gelatin to a concentration of 7.5×10^5 in 4 mL. Plants were spray inoculated with the suspension using an artist's airbrush. Barley plants were 1 week old at the time of inoculation, and virulence was assessed 5 days after inoculation; rice and weeping lovegrass plants were 2 weeks old at the time of inoculation, and virulence was assessed 1 week after inoculation.

For quantification of fungal virulence, 4-inch pots containing 10 to 15 barley plants were grown for 10 days before inoculation. The prolonged incubation time allowed for full emergence of the cotyledons. A lower concentration of conidia (7.5×10^4 in 3 mL) was used for spraying to allow formation of individual disease lesions. Five days after inoculation, cotyledons were scored for lesions with a severity of type 2 or greater, according to the scale of Valent et al. (1991). Cotyledons were scored in this assay rather than true leaves, because they exhibited minimal growth during the course of the assay and were of a relatively uniform surface area (7.4 ± 2 cm^2; $n = 10$

Table 4. Plasmids Used in This Study

Name	Description/Reference
pCB1004	Modified *HPH* gene in pBC SK+ used for insertional mutagenesis (Carroll et al., 1994)
pCB1220	λ Barfix plasmid with a 13-kb 4091-5-8 genomic DNA insert; identified by complementation of the *pth11* mutant K261 (Sweigard et al., 1998)
pCB1221	λ Barfix plasmid with a 9-kb 4091-5-8 genomic DNA insert; identified by complementation of the *pth11* mutant K364 (Sweigard et al., 1998)
pCB1264	pBluescript II SK− with Bialophos resistance marker at the SspI site
pCB1272	6.5-kb ApaI-EcoRI fragment from pCB1221 in pCB1264
pCB1278	4.7-kb HindIII fragment from pCB1220 in pCB1264
pCB1303	pCB1272 with the 3′ SstI-EcoRI fragment removed to yield a 4.3-kb ApaI-SstI subclone carrying the full-length *PTH11* gene
pCB1312	2.4-kb *PTH11* cDNA from λ ZipLox cDNA library of strain 6043; identified by hybridization with the pCB1278 4.7-kb HindIII fragment
pCB1313	2.1-kb *PTH11* cDNA from λ ZipLox cDNA library of strain 6043; identified by hybridization with the pCB1278 4.7-kb HindIII fragment
pCB1314	1.0-kb *PTH11* cDNA from λ ZipLox cDNA library of strain 6043; identified by hybridization with the pCB1278 4.7-kb HindIII fragment
pCB1315	1.6-kb *PTH11* cDNA from λ ZipLox cDNA library of strain 6043; identified by hybridization with the pCB1272 6.5-kb ApaI-EcoRI fragment
pCB1397	λ NFSFix plasmid with a 10.6-kb 4091-5-8 genomic DNA insert; identified by hybridization with the *PTH11* cDNA from pCB1312
pCB1399	λ NFSFix plasmid with a 14.5-kb 4091-5-8 genomic DNA insert; identified by hybridization with the *PTH11* cDNA from pCB1312
pCB1400	*PTH11* gene disruption vector; the SpeI-KpnI fragment in the *PTH11* ORF of pCB1397 replaced with an XbaI-KpnI fragment carrying the *HPH* gene from pCSN43 (Staben et al., 1989)
pCB1401	*PTH11* gene disruption vector; the SpeI-KpnI fragment in the *PTH11* ORF of pCB1399 replaced with an XbaI-KpnI fragment carrying the *HPH* gene from pCSN43 (Staben et al., 1989)
pCB1530	pBluescript II SK− carrying the Bialophos resistance marker (Sweigard et al., 1997)
pCB1621	Plasmid rescued by BglII digestion of genomic DNA from *pth11* mutant K261
pCB1622	Plasmid rescued by BamHI and BglII digestion of genomic DNA from *pth11* mutant K364
pSM79	λ NFSFix plasmid with a G-11 genomic DNA insert; identified by hybridization with the *PTH11* cDNA from pCB1312
pSM85	λ NFSFix plasmid with a G-207 genomic DNA insert; identified by hybridization with the *PTH11* cDNA from pCB1312
pSM111	ApaI-NotI *PTH11–FLAG* fragment in pRS424 (Sikorski and Heiter, 1989); the *PTH11–FLAG* fragment contains 0.9 kb of the *PTH11* promoter, *PTH11* fused to the *FLAG* epitope at the last codon, and 0.5 kb of the *PTH11* 3′ untranslated region
pSM131	pSM111 with *FLAG* replaced by *GFP*: constructed by gap repair in *S. cerevisiae*, as described by Oldenburg et al. (1997)
pSM141	0.5-kb promoter of the P2 ribosomal protein gene fused to *GFP* (0.7-kb fragment) in pCB1264
pSM151	0.5-kb promoter of the P2 ribosomal protein gene fused to *PTH11–GFP* in pCB1264

cotyledons). The experiment was performed in duplicate, and the results from both tests were pooled.

For leaf appressorium assays, 8- to 14-day-old barley leaves were taped adaxial side down to the bottom of Petri dishes using double-sided tape. Twenty-five-microliter drops containing ~1250 condia were placed on the leaves ~2 cm apart. This conidium concentration was also used for in vitro appressorium assays on the hydrophilic side of GelBond (FMC BioProducts, Rockland, ME), polystyrene (Corning Glass Works, Corning, NY), and Teflon (Dupont, Wilmington, DE). The Petri dishes containing the leaves were kept in a moist chamber at room temperature for 16 to 24 hr, and the inoculated leaf sections were then excised, fixed, and decolorized in an ethanol–acetic acid (2:1) solution at room temperature for 1 hr. Visualization of germlings on the leaf surface was facilitated by staining for 5 min with 0.1% trypan blue in lactophenol (lactic acid–phenol–glycerol [1:1:1]) followed by a brief rinse in lactophenol. The stained leaf sections were then mounted in lactophenol for microscopy. This staining regimen was not used for assays with strain CP987 and its derivatives because lactophenol disrupted attachment of these strains to the leaf surface. This was probably due to the failure of these strains to produce spore tip mucilage, which is important for adhesion (Hamer et al., 1988). CP987 and its derivatives were stained with a buffered solution of aniline blue and then destained and mounted in water. Where indicated, cAMP was added to a final concentration of 10 mM from a 50 mM aqueous stock, the diacylglycerol 1,2-dioctanoyl-*rac*-glycerol was added to a final concentration of 20 μg/mL from a 10 mg/mL DMSO stock, and the plant cutin monomer 1,16-hexadecanediol was added to a final concentration of 2 μg/mL from a 0.5 mg/mL DMSO stock.

Microscopy

The images shown in Figure 4 were photographed with a 100× oil immersion objective (NA 1.3) using a Zeiss Axiophot microscope (Carl Zeiss, Inc., Thornwood, NY). Digitized confocal images were acquired at 1024 × 1024 pixel resolution with a 100× oil immersion objective (NA 1.4) using a Zeiss model LSM410 laser scanning microscope. For visualization of infection hyphae, barley leaves (cv BarSoy) were inoculated as described for the leaf appressorium assays and incubated for 112 hr. The tissue was then prepared for aniline blue epifluorescence, as described by Hood and Shew (1996),

using the modifications described by Urban et al. (1999). The prepared tissue was imaged using 364-nm excitation from a Coherent Enterprise UV Ar laser (Coherent, Inc., Santa Clara, CA) and a 400-nm longpass emission filter. For Pth11–GFP localization, the synthetic GFP isoform described by Sheen et al. (1995) was used. Conidia were resuspended in defined complex medium containing 2 μg/mL 1,16-hexadecanediol. These conditions supported vegetative growth of germlings after appressorium differentiation, whereas resuspension in water supplemented with 1,16-hexadecanediol did not. Because we were able to detect Pth11–GFP only after the transition to vegetative growth, water supplemented with 1,16-hexadecanediol was inadequate for these experiments. Fifty-microliter drops containing ~1250 conidia were inoculated on the surface of a Lab-Tek II chambered No. 1.5 coverglass system (Nalge Nunc International, Naperville, IL) and incubated in a moist environment at room temperature for 24 hr. The cells were imaged using 488-nm excitation from an Ar-Kr laser (Omnichrome, Chino, CA) and a 500-nm longpass emission filter. Germlings expressing Pth11–GFP and Pth11 fused to the FLAG epitope (Eastman Kodak, New Haven, CT) were imaged under identical brightness/contrast, laser power, and pinhole settings. These setting were optimized for imaging of germlings expressing GFP.

ACKNOWLEDGMENTS

We acknowledge Phil Smith and Kathy Kline-Smith for maintaining an excellent plant growth facility. We thank Jim Steffens, Guo-Hua Miao, Yulin Jia, Gregory T. Bryan, Timothy M. Bourett, and Richard J. Howard for comments on portions of the manuscript and the anonymous reviewers for their helpful advice. We are indebted to Richard J. Howard and Timothy M. Bourett for assistance with the microscopy and stimulating discussions.

Received June 21, 1999; accepted August 11, 1999.

REFERENCES

Adachi, K., and Hamer, J. (1998). Divergent cAMP signaling pathways regulate growth and pathogenesis in the rice blast fungus *Magnaporthe grisea*. Plant Cell **10,** 1361–1373.

Antonsson, B., Montessuit, S., Friedii, L., Payton, M.A., and Paravicini, G. (1994). Protein kinase C in yeast, characteristics of the *Saccharomyces cerevisiae PKC1* gene product. J. Biol. Chem. **269,** 16821–16828.

Beckerman, J., and Ebbole, D. (1996). *MPG1*, a gene encoding a fungal hydrophobin of *Magnaporthe grisea*, is involved in surface recognition. Mol. Plant-Microbe Interact. **9,** 450–456.

Bockaert, J., and Pin, J.P. (1999). Molecular tinkering of G protein–coupled receptors: An evolutionary success. EMBO J. **18,** 1723–1729.

Bourett, T., and Howard, R. (1990). In vitro development of penetration structures in the rice blast fungus *Magnaporthe grisea*. Can. J. Bot. **69,** 329–342.

Carroll, A., Sweigard, J., and Valent, B. (1994). Improved vectors for selecting resistance to hygromycin. Fungal Genet. Newslett. **41,** 22.

Choi, W., and Dean, R. (1997). The adenylate cyclase gene *MAC1* of *Magnaporthe grisea* controls appressorium formation and other aspects of growth and development. Plant Cell **9,** 1973–1983.

Crawford, M.S., Chumley, F.G., Weaver, C.G., and Valent, B. (1986). Characterization of the heterokaryotic and vegetative diploid phases of *Magnaporthe grisea*. Genetics **114,** 1111–1129.

Gilbert, R., Johnson, A., and Dean, R. (1996). Chemical signals responsible for appressorium formation in the rice blast fungus *Magnaporthe grisea*. Physiol. Mol. Plant Pathol. **48,** 335–346.

Gudermann, T., Kalkbrenner, F., and Schultz, G. (1996). Diversity and selectivity of receptor–G protein interaction. Annu. Rev. Pharmacol. Toxicol. **36,** 429–459.

Hamer, J.E., Howard, R.J., Chumley, F.G., and Valent, B. (1988). A mechanism for surface attachment in spores of a plant pathogenic fungus. Science **239,** 288–290.

Hicke, L. (1999). Gettin' down with ubiquitin: Turning off cell-surface receptors, transporters and channels. Trends Cell Biol. **9,** 107–112.

Hicke, L., Zanolari, B., and Riezman, H. (1998). Cytoplasmic tail phosphorylation of the α-factor receptor is required for its ubiquitination and internalization. J. Cell. Biol. **141,** 349–358.

Hoch, H.C., Staples, R.C., Whitehead, B., Comeau, J., and Wolf, E.D. (1987). Signaling for growth orientation and cell differentiation by surface topography in *Uromyces*. Science **235,** 1659–1662.

Hofman, K., and Stoffel, W. (1993). TMbase—A database of membrane spanning protein segments. Biol. Chem. Hoppe-Seyler **347,** 166.

Hood, M.E., and Shew, H.D. (1996). Applications of KOH-aniline blue fluorescence in the study of plant–fungal interactions. Phytopathology **86,** 704–708.

Howard, R. (1994). Cell biology of pathogenesis. In Rice Blast Disease, R. Zeigler, S. Leong, and P. Teng, eds (Singapore: CAB International), pp. 3–22.

Howard, R., Ferrari, M., Roach, D., and Money, N. (1991). Penetration of hard substrates by a fungus employing enormous turgor pressures. Proc. Natl. Acad. Sci. USA **88,** 11281–11284.

Kershaw, M.J., and Talbot, N.J. (1998). Hydrophobins and repellents: Proteins with fundamental roles in fungal morphogenesis. Fungal Gen. Biol. **23,** 18–33.

Kolattukudy, P., Rogers, L., Li, D., Hwang, C., and Flaishman, M. (1995). Surface signaling in pathogenesis. Proc. Natl. Acad. Sci. USA **92,** 4080–4087.

Lee, Y.-H., and Dean, R. (1993). cAMP regulates infection structure formation in the plant pathogenic fungus *Magnaporthe grisea*. Plant Cell **5,** 693–700.

Lee, Y.-H., and Dean, R. (1994). Hydrophobicity of contact surface induces appressorium formation in *Magnaporthe grisea*. FEMS Microbiol. Lett. **115,** 71–76.

Leung, H., Borromeo, E., Bernardo, M., and Notteghem, J. (1988). Genetic analysis of virulence in the rice blast fungus *Magnaporthe grisea*. Phytopathology **78,** 1227–1233.

Liu, S., and Dean, R. (1997). G protein α subunit genes control growth, development, and pathogenicity of *Magnaporthe grisea*. Mol. Plant-Microbe Interact. **10,** 1075–1086.

Mitchell, T., and Dean, R. (1995). The cAMP-dependent protein kinase catalytic subunit is required for appressorium formation and pathogenesis by the rice blast pathogen *Magnaporthe grisea*. Plant Cell **7,** 1869–1878.

Oldenburg, K.R., Vo, K.T., Michaelis, S., and Paddon, C. (1997). Recombination-mediated PCR-directed plasmid construction *in vivo* in yeast. Nucleic Acids Res. **25,** 451–452.

Ou, S. (1985). Rice Diseases, 2nd ed. (Kew, UK: Commonwealth Mycological Institute).

Podila, G.K., Rogers, L.M., and Kolattukudy, P.E. (1993). Chemical signals from avocado surface wax trigger germination and appressorium formation in *Colletotrichum gloeosporioides*. Plant Physiol. **103,** 267–272.

Sambrook, J., Fritsch, E., and Maniatis, T. (1989). Molecular Cloning: A Laboratory Manual, 2nd ed. (Cold Spring Harbor, NY: Cold Spring Harbor Laboratory Press).

Schafer, W. (1994). Molecular mechanisms of fungal pathogenicity to plants. Annu. Rev. Phytopathol. **32,** 461–477.

Scheistel, R., Dominska, M., and Petes, T. (1993). Transformation of *Saccharomyces cerevisiae* with nonhomologous DNA: Illegitimate integration of transforming DNA into yeast chromosomes and in vivo ligation of transforming DNA to mitochondrial DNA sequences. Mol. Cell. Biol. **13,** 2697–2705.

Sheen, J., Hwang, S., Niwa, Y., Kobayashi, H., and Galbraith, D.W. (1995). Green fluorescent protein as a new vital marker in plant cells. Plant J. **8,** 101–108.

Sikorski, R.S., and Heiter, P. (1989). A system of shuttle vectors and yeast host strains designed for efficient manipulation of DNA in *Saccharomyces cerevisiae*. Genetics **122,** 19–27.

Staben, C., Jensen, B., Singer, M., Pollock, J., Schechtman, M., Kinsey, J., and Selker, E. (1989). Use of a bacterial hygromycin B resistance gene as a dominant selectable marker in *Neurospora crassa* transformation. Fungal Genet. Newslett. **36,** 79–81.

Sweigard, J., Carroll, A., Kang, S., Farrall, L., Chumley, F., and Valent, B. (1995). Identification, cloning, and characterization of *PWL2*, a gene for host species specificity in the rice blast fungus. Plant Cell **7,** 1221–1233.

Sweigard, J., Chumley, F., Carroll, A., Farrall, L., and Valent, B. (1997). A series of vectors for fungal transformation. Fungal Genet. Newslett. **44,** 52–53.

Sweigard, J., Carroll, A., Farrall, L., Chumley, F., and Valent, B. (1998). *Magnaporthe grisea* pathogenicity genes obtained through insertional mutagenesis. Mol. Plant-Microbe Interact. **11,** 404–412.

Talbot, N.J. (1995). Having a blast: Exploring the pathogenicity of *Magnaporthe grisea*. Trends Microbiol. **3,** 9–16.

Talbot, N.J., Kershaw, M., Wakley, G., de Vries, O., Wessels, J.G.H., and Hamer, J.E. (1996). *MPG1* encodes a fungal hydrophobin involved in surface interactions during infection-related development by *Magnaporthe grisea*. Plant Cell **8,** 985–989.

Thines, E., Eilbert, F., Sterner, O., and Anke, H. (1997). Signal transduction leading to appressorium formation in germinating conidia of *Magnaporthe grisea*: Effects of second messengers diacylglycerols, ceramides and spingomyelin. FEMS Microbiol. Lett. **156,** 91–94.

Urban, M., Bhargava, T., and Hamer, J.E. (1999). An ATP-driven drug efflux pump is a novel pathogenicity factor in rice blast disease. EMBO J. **18,** 512–521.

Valent, B. (1997). The rice blast fungus, *Magnaporthe grisea*. In The Mycota, G.C. Carroll and P. Tuzynski, eds (Berlin: Springer-Verlag), pp. 37–54.

Valent, B., and Chumley, F. (1987). Genetic analysis of host species specificity in *Magnaporthe grisea*. Univ. Calif. Los Angeles Symp. Mol. Cell. Biol. **48,** 83–93.

Valent, B., Farrall, L., and Chumley, F. (1991). *Magnaporthe grisea* genes for pathogenicity and virulence identified through a series of backcrosses. Genetics **127,** 87–101.

Van der Plank, J.E. (1975). Principles of Plant Infection. (New York: Academic Press).

Watanabe, M., Chen, C.-Y., and Levin, D.E. (1994). *Saccharomyces cerevisiae PKC1* encodes a protein kinase C (PKC) homolog with a substrate specificity similar to that of mammalian PKC. J. Biol. Chem. **269,** 16829–16836.

Xiao, J.-Z., Watanabe, T., Kamakura, T., Ohshima, A., and Yamaguchi, I. (1994). Studies on cellular differentiation of *Magnaporthe grisea*. Physicochemical aspects of substratum surfaces in relation to appressorium formation. Physiol. Mol. Plant Pathol. **44,** 227–236.

Xu, J.-R., and Hamer, J. (1996). MAP kinase and cAMP signaling regulate infection structure formation and pathogenic growth in the rice blast fungus *Magnaporthe grisea*. Genes Dev. **10,** 2696–2706.

Xu, J.-R., Urban, M., Sweigard, J., and Hamer, J. (1997). The *CPKA* gene of *Magnaporthe grisea* is essential for appressorial penetration. Mol. Plant-Microbe Interact. **10,** 187–194.

Xu, J.-R., Staiger, C., and Hamer, J. (1998). Inactivation of the mitogen-activated protein kinase Mps1 from the rice blast fungus prevents penetration of host cells but allows activation of plant defense responses. Proc. Natl. Acad. Sci. USA **95,** 12713–12718.